IEEE Access
Multidisciplinary | Rapid Review | Open Access Journal

Received 18 December 2023, accepted 22 January 2024, date of publication 14 February 2024, date of current version 23 February 2024.

Digital Object Identifier 10.1109/ACCESS.2024.3366448

RESEARCH ARTICLE

Optoelectronic Heterodyne THz Receiver for 100–300 GHz Communication Links

MILAN DEUMER[1], OLIVER STIEWE[1], SIMON NELLEN[1], SEBASTIAN LAUCK[1], STEFFEN BREUER[1], ROBERT B. KOHLHAAS[1], COLJA SCHUBERT[1], ROBERT ELSCHNER[1], (Member, IEEE), RONALD FREUND[1,2], AND MARTIN SCHELL[1,3], (Member, IEEE)

[1]Fraunhofer Heinrich Hertz Institute, 10587 Berlin, Germany
[2]Institute for Telecommunication Systems, Technische Universität Berlin, 10623 Berlin, Germany
[3]Institute for Solid State Physics, Technische Universität Berlin, 10623 Berlin, Germany

Corresponding author: Milan Deumer (milan.deumer@hhi.fraunhofer.de)

This work was supported in part by TERAWAY Project funded by European Union's Horizon 2020 Research and Innovation (R&I) Programme under Grant 871668, in part by the Initiative of Photonics Public Private Partnership (PPP), and in part by the Project 6G SENTINEL funded by Fraunhofer Gesellschaft e.V. für Angewandte Forschung.

ABSTRACT Terahertz wireless communications is an increasingly interesting research topic due to the high demand for un-allocated channels and high data rates. Photonic solutions have shown great potential in this field. However, most photonics assisted THz links so far have employed optoelectronics only on the transmit side. Thus, the full potential of photonic THz communication has not been utilized yet. Here, we introduce optoelectronics also on the receive side by using a photoconductive antenna based heterodyne THz detector. This allows down-conversion of data signals from the W-, D-, and THz-band to the baseband using a laser beat signal as local oscillator. Using electromagnetic modeling, we designed passive radio frequency structures and a receiver package to handle high intermediate frequency output signals. In a homodyne spectroscopic setup, the receiver shows a frequency response superior to state-of-the-art photoconductive antennas due to an improved photoconductive material. In a heterodyne testbed, the receiver exhibits a large intermediate frequency bandwidth of 11 GHz and a conversion gain of -47 dB. This enabled us to employ the receiver in a fully photonic wireless link at sub-terahertz and terahertz frequencies together with a PIN photodiode emitter. We achieved error-free transmission of 4-QAM signals with gross data rates up to 12 Gbit/s at carrier frequencies up to 320 GHz. This work shows the huge potential of optoelectronic receivers for THz wireless communications and enables the exploration of full photonic THz links.

INDEX TERMS Heterodyne receiver, photoconductive antenna, photonic terahertz link, millimeter-wave, mmWave, terahertz, terahertz communication, wireless communication.

I. INTRODUCTION

In recent years, (sub-) terahertz (THz) frequencies between 100 GHz and 1 THz have gained a lot of interest for application in high-data-rate wireless communication links due to the high available bandwidth in these frequency bands [1], [2], [3], [4], [5], [6], [7], [8]. In particular, the frequency band between 100 and 300 GHz is very promising, as it contains several windows with low atmospheric attenuation [9]. This allows for higher transmission distances up to more than a kilometer [3], [10]. Hence, channels up to 320 GHz have been standardized for wireless communication by IEEE 802.15.3d [11], [12]. However, it is hard to generate THz carrier frequencies, as they are very high for electronic oscillators and very low for purely optical sources such as lasers. Nonetheless, both electronic and photonic THz links have been demonstrated. Electronic solutions, due to their high output power still the dominant technology per today, need to employ multiple mixer stages for frequency up-conversion [3], [10], [13], [14]. On the other hand, photonic solutions employ single step photomixing for down-conversion from the optical-domain to the

The associate editor coordinating the review of this manuscript and approving it for publication was Bilal Khawaja.

THz-domain. The photonic approach benefits from the huge bandwidth in the optical-domain, the potentially low phase noise of optically generated signals, and the possibility to integrate the wireless links directly with existing optical fiber networks. Consequently, photonic assisted THz links have recently gained increasing research interest. The majority of such links employed a photomixer, such as a PIN or UTC photodiode (PD), as transmitter (Tx) and an electronic receiver (Rx) [2], [6], [9], [15]. To fully utilize the aforementioned benefits of photonic THz links, photomixers need to be used at both the transmitter and receiver side. So far, only very few such links have been demonstrated since photonic THz receivers typically exhibit only low conversion gain and a low intermediate frequency (IF) bandwidth. In [16], a commercially available photoconductive antenna (PCA) was used as receiver together with a PIN PD emitter. Here, transmission of 100 Mbit/s binary phase shift keying (BPSK) signals over a link distance of 25 cm at carrier frequencies between 80 and 320 GHz was achieved. In [2] the authors employed a UTC PD to transmit quadrature phase shift keying (QPSK) signals over 58 m towards a receiver comprised of an electronic THz amplifier and a PCA detector. In this case, data rates up to 10 Gbit/s for a single channel and 30 Gbit/s using 20 aggregated 1.5 Gbit/s channels were achieved for carriers up to 340 GHz.

In this work, we present a photoconductive THz receiver specifically designed for communication applications. This receiver is suitable for carrier frequencies between 100 and 320 GHz and shows an IF bandwidth of 11 GHz. With this receiver and a state-of-the-art PIN PD as transmitter, we demonstrate a fully photonic THz communication link.

In the remainder of this paper, we describe the design of the photoconductive receiver and demonstrate its capabilities in a fully photonic link with up to 12 Gbit/s data rate over a link distance of 1 m at carrier frequencies between 100 to 320 GHz. These are the highest reported data rates for a fully photonic THz link without using electronic THz amplifiers.

II. RECEIVER DESIGN

A. PHOTOCONDUCTIVE ANTENNA

The presented heterodyne receiver is similar to a state-of-the-art THz PCA [17] used for spectroscopy and consists of an ultrafast iron-doped indium gallium arsenide (InGaAs:Fe) photoconductor grown by molecular beam epitaxy on a semi-insulating indium phosphide (InP) substrate. This material provides ultra-short charge carrier lifetime, high carrier mobility and high resistivity, which is necessary for broadband and low noise operation. The photoconductor is connected to a bow-tie antenna through interdigitated gold finger contacts [17] as seen in Fig. 1(c). This self-complimentary antenna type is commonly used in optoelectronic THz emitters and receivers because it offers ultra-high bandwidths and linear polarization. Although other antennas such as dipoles offer higher impedances at resonance that match the photoconductor's impedance better, these resonant antennas are not suitable for the target frequency range between 100 and 300 GHz.

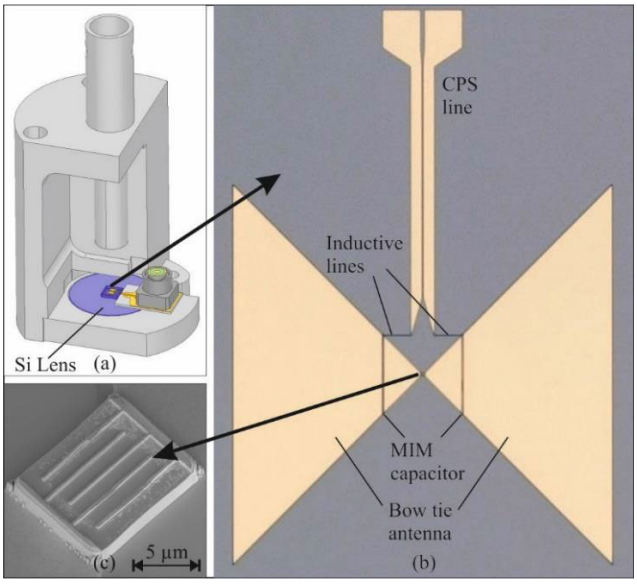

FIGURE 1. The HFSS model used for full-wave simulations of the packaged chip (a), a micrograph of the PCA chip (b) and a scanning electron micrograph of the interdigitated fingers on the photoconductive mesa (c).

The PCA device acts as a mixer that uses an optical beat note as a photonic local oscillator (LO) to down-convert THz electromagnetic waves incident on the antenna. The beat note is generated by superimposing two laser lines and therefore has the beat frequency $f_{LO,Rx} = |f_{Laser1} - f_{Laser2}|$. This optical intensity beating modulates the conductance of the photoconductive element. The THz wave captured by the antenna, on the other hand, generates a voltage across the photoconductor. Consequently, the current flowing through the PCA is the product of the oscillating conductance and voltage and therefore contains a spectral component with the difference frequency of THz wave and the Rx LO, $f_{IF} = |f_{THz} - f_{LO,Rx}|$. The latter component of the signal is proportional to the THz signal amplitude and can be measured at the output of the device with conventional electronics.

B. RF WAVEGUIDES AND PACKAGE

For THz spectroscopy, the transmitter emits a single tone and the photonic LO frequency at the receiver is chosen equal or close to that frequency so that a (quasi) DC signal is measured at the output of the receiver. In contrast, for THz communications, the transmitter will not only emit a single tone but a broadband data signal, i.e. sidebands around the carrier frequency with a bandwidth depending on the data rate and modulation format. These sidebands are then also present in the down-converted signal. Thus, for multi-Gbit/s data rates, the receiver output also contains signals with several GHz bandwidth. Furthermore, the transmitter and receiver are often operated at an IF spacing of several GHz. Therefore, a THz PCA receiver for data communications

has to be capable of guiding these radio frequency (RF) signals from the PCA to its output. Thus, RF waveguides and matching structures to the chip and package are needed. However, since the impedance of the PCA is typically very high, i.e. several kΩ, broadband matching is not possible in real devices. Therefore, we focused on the RF waveguide structures in our PCA design, which we developed using Ansys HFSS. Due to the two-terminal contact structure of the PCA we chose to implement a coplanar stripline (CPS) on the chip with an impedance of 50 Ω to match the external circuitry. In order to eliminate the influence of the THz bow-tie antenna on the RF output signal propagation, we also inserted metal-insulator-metal (MIM) capacitors between the antenna wings and the photoconductor contacts. The capacitor size was chosen so that it acts as an open circuit for the RF signals and as a short circuit for signals in the THz frequency range. Therefore, the antenna works as intended for the carrier frequencies and has little impact on the down-converted data signals. Additionally, we introduced thin metal strips perpendicular to the CPS at the transition between the PCA and the CPS. These strips show inductive behavior, i.e. their impedance increases with frequency. This way the influence of the CPS line on the antenna performance in the THz range can be reduced while introducing only a minor disturbance for the IF signals. A micrograph of the resulting chip is shown in Fig. 1(b). We then developed a package around the chip, which is depicted in Fig. 1(a). The chip was placed on a hyper-hemispherical silicon lens and connected to a gold-coated ceramic via bondwires. On the ceramic, we implemented a CPS to coplanar waveguide (CPW) transition and a footprint for an RF coaxial connector. The package furthermore contains a mounting for the optical fiber that is used to illuminate the PCA.

C. CHARACTERIZATION

The key parameters to characterize the performance of our receiver are its photo-conductance, THz carrier and IF frequency response as well as its noise and conversion gain.

1) PHOTO-CONDUCTANCE

To obtain the photo-conductance, we first measured the DC current-voltage characteristics of the PCA. To this end, we drove the receiver with an optical power between 5 and 40 mW and applied DC biases between −0.05 V and +0.05 V around operating point of 0 V. We then measured the current and subtracted the dark current to obtain the pure photo-response. The slope of the resulting I-V-curve gives the photo-conductance for each particular optical power. Fig. 2 shows the photo-conductance over the optical power incident on the PCA. Note that the photo-response of the PCA is linear up to 40 mW (16 dBm) optical input power.

2) THZ FREQUENCY RESPONSE

We then measured the frequency responses of the receiver using the setup shown in Fig. 3(a). Here, we aligned the receiver with a commercially available PIN PD emitter via

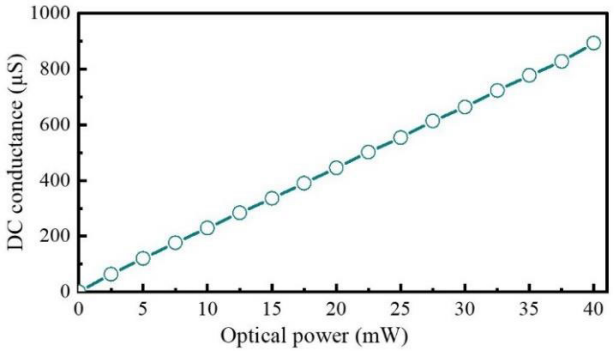

FIGURE 2. Photo-conductance of the PCA at a DC bias of 0 V. The conductance shows a linear dependence on the optical excitation.

two off-axis parabolic mirrors over a path length of approximately 30 cm. Both the Tx and Rx were driven with 30 mW of the same optical beating generated by two C-band lasers. A phase modulation technique is used to acquire the received signal via lock-in amplification (LIA) [18], [19]. Fig. 4 shows the resulting coherent homodyne THz spectrum between 50 GHz and 4.5 THz. Our novel receiver shows a frequency response very similar to conventional state-of-the-art PCAs [17]. Due to the higher carrier mobility and lifetime of the photoconductive material employed for the heterodyne receiver, it even shows a slightly higher signal amplitude at frequencies below 1.5 THz compared to the reference Rx. From the spectra, it can also be seen that this comes at the cost of a slightly higher noise level and a lower spectroscopic bandwidth of only approx. 4 THz. However, for the application in a communications link below 300 GHz the increased signal amplitude is highly beneficial.

3) INTERMEDIATE FREQUENCY RESPONSE

We then used the setup in Fig. 3(b) to evaluate the IF performance of our receiver. This time, we aligned the Tx and Rx over a distance of 1 m using parabolic mirrors. In contrast to the homodyne setup, the emitter and detector were driven with separate beat notes generated by three lasers, i.e. $f_{Tx} = |f_{L1}\text{-}f_{L2}|$ and $f_{Rx} = |f_{L3}\text{-}f_{L2}|$. The frequency of the two beatings was tuned individually to obtain a signal with the desired IF $f_{IF} = |f_{Tx}\text{-}f_{Rx}| = |f_{L1}\text{-}f_{L3}|$ at the receiver, which was then fed to a low noise amplifier (LNA, Minicircuits ZVA213S+) with 26 dB gain. We used an electrical spectrum analyzer (ESA) to evaluate the IF signal power. Fig. 5 shows the resulting IF spectra for 30 mW and 40 mW of optical excitation at the Tx and Rx, respectively. The measurement results show an excellent agreement with the HFSS simulation, which was fitted only by introducing an offset to compensate for the internal conversion efficiency of the PCA. It can also be seen that a 3 dB bandwidth of 11 GHz was achieved with this device. The noise level shown in Fig. 5 was measured by blocking the THz path. However, no change in the noise floor was observed when the receiver was disconnected. This suggests that the noise of our link is dominated

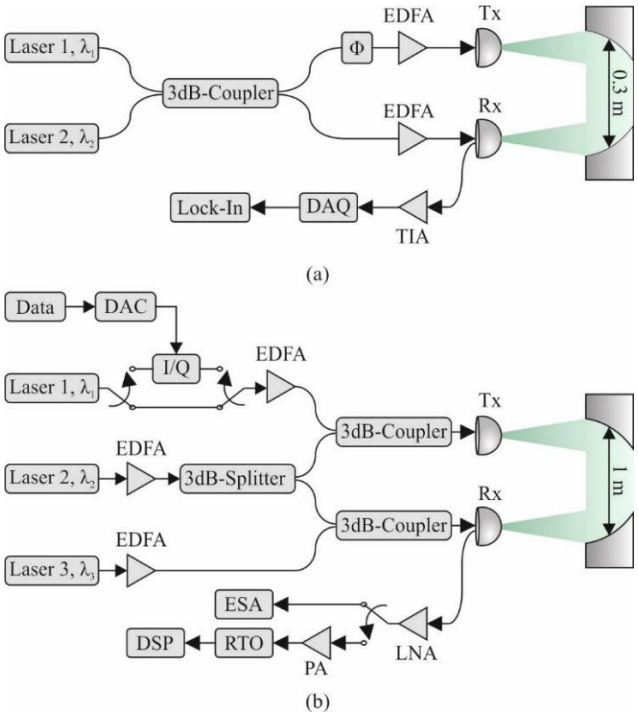

FIGURE 3. Measurement setups used for the characterization of the heterodyne receiver. In the homodyne configuration (a), two lasers are used to generate one optical beating for both Tx and Rx. In the heterodyne configuration (b), three lasers generate two separate beatings for the Tx and Rx. For data transmission, we inserted a modulator after laser 1 and replaced the ESA with an RTO and a DSP.

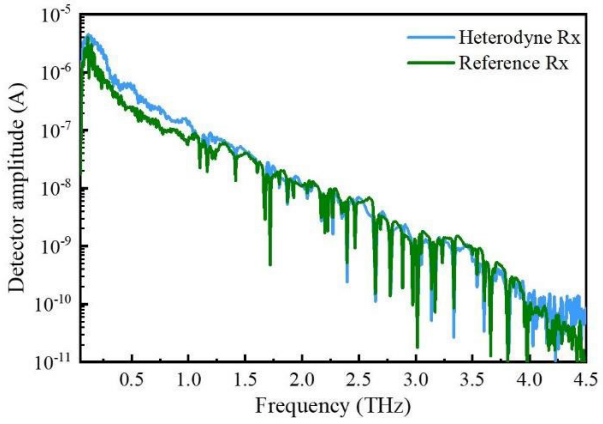

FIGURE 4. Measured THz spectra using a PIN photodiode as transmitter and the novel PCA as receiver in a homodyne system configuration. As can be seen, the heterodyne receiver shows slightly less bandwidth than the reference device [17] but has a higher signal amplitude for frequencies below 1.5 THz.

by subsequent electronics, i.e. the amplifier or the ESA itself. Hence, we could not access the actual IF noise of our device with the available instruments.

4) CONVERSION GAIN

The conversion gain of the receiver is defined by the ratio of the IF signal power present before the amplifier and the THz power incident on the device. To this end, we measured the

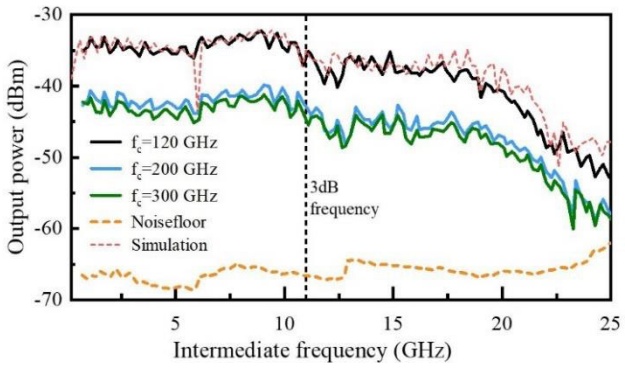

FIGURE 5. Measured IF spectra of the heterodyne receiver for different THz carrier frequencies f_c and electrical simulation results. The Tx and Rx were driven with 30 and 40 mW of optical power, respectively.

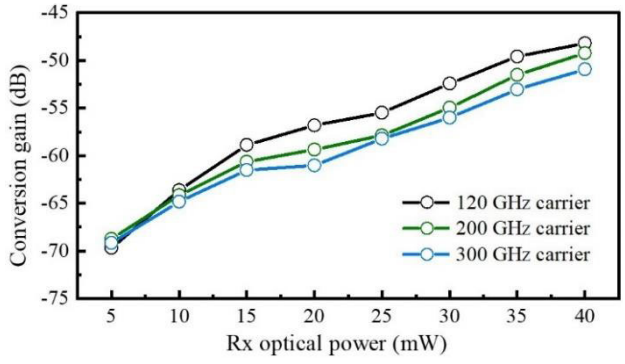

FIGURE 6. Conversion gain of the heterodyne PCA receiver for different optical LO powers and carrier frequencies.

Rx output signal at a fixed IF of 8 GHz for various optical LO powers at THz carrier frequencies of 120, 200 and 300 GHz. We then obtained the conversion gain by dividing these powers by the output power of our emitter, which we measured with a calibrated pyroelectric detector [20], [21]. The results in Fig. 6 show a strong increase in conversion gain between 18 and 20 dB over the considered optical powers from 5 to 40 mW, with a maximum of −47 dB. The IF power P_{IF} and thus the conversion gain scales with the square of power P_{opt} at the Rx:

$$P_{IF} = I_{IF}^2 R \propto G_{PCA}^2 \propto P_{opt}^2 \tag{1}$$

Here, I_{IF} is the IF output current and G_{PCA} is the photo-conductance of the receiver. Fig. 2 shows a 9-fold increase in conductance when the optical excitation power is increased from 5 to 40 mW. This increase in conductance is expected to result in a 19 dB increase in conversion gain, which is consistent with our measurements. Additionally, we observed a minimal frequency roll-off in conversion gain, with only a 2.7 dB decrease between 120 and 300 GHz at 40 mW of excitation power.

In summary, the characterization results show that our novel receiver not only provides a large IF bandwidth that can support high-bandwidth communication channels but also

outperforms conventional PCA detectors in the frequency band between 100 and 300 GHz.

III. FULLY PHOTONIC THZ LINK

After characterizing the receiver, we test its performance in an actual data link. To this end, we modified the setup in Fig. 3(b) to allow for the transmission of data signals and then investigated the impact of different optical driving parameters, carrier frequencies, and symbol rates.

A. LINK SETUP

1) DATA MODULATION

As shown in Fig. 3 (b), we added an inphase-quadrature (I-Q) modulator ($LiNbO_3$, 3-dB analog bandwidth = 25 GHz, extinction ratio = 40 dB) into the setup between laser 1 and its EDFA in order to modulate QPSK signals with data rates between 2 and 6 GBd on the optical carrier. A high-speed digital-to-analog converter (CMOS-based DAC, 8-bit resolution, sampling rate = 84 GS/s, 3-dB analog bandwidth = 20 GHz) served to drive the modulator with a repeated random bit pattern sequence. This pattern contained 8192 root raised cosine (RRC) shaped symbols including a header for frame synchronization, carrier offset estimation and channel estimation.

2) DIGITAL SIGNAL PROCESSING

For capturing the received signals, we added another 20 dB power amplifier after the LNA and replaced the ESA with a real-time oscilloscope (RTO, Tektronix DPO72004). Applying digital signal processing (DSP) then allowed us to recover the transmitted data. To this end, we employed a training-aided single-carrier DSP [22], originally used in high-capacity dual-polarization fiber-optical communications, as Tx and Rx DSP. It contains blocks for frontend corrections, training-aided frame synchronization, frequency offset estimation, and channel estimation as well as T/2-spaced frequency-domain equalization. This is followed by a carrier-phase estimation (CPE) using the blind phase search algorithm, and T-spaced adaptive equalization using a decision-directed, real-valued 4 × 4 equalizer. For each measurement, we evaluated more than one million samples of the bit pattern sequence to estimate the bit error rate (BER) and generate a constellation diagram.

B. EXPERIMENTS

1) OPTICAL DRIVING PARAMETERS

In order to maximize the data rate, we investigated the influence of the optical excitation in the Tx and Rx on the signal quality. Starting with the impact of the Tx photocurrent, which is proportional to the emitter THz power, we distinguish between two contributions to the photocurrent in the PD: i) the current generated by the unmodulated laser line, i.e. laser 2, and ii) the resulting current from the modulated laser line, i.e. laser 1. The respective current contribution is measured by switching off the other laser. In the following,

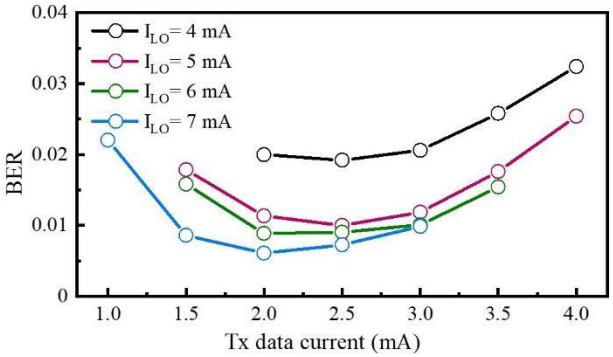

FIGURE 7. Measured BER for various driving currents in the Tx. The carrier frequency, data rate and RX LO power were set to 120 GHz, 10 Gbit/s and 40 mW, respectively. The BER shows a minimum for data currents much lower than the LO current.

we will refer to the current from i) as Tx LO current (I_{LO}) since the unmodulated line serves as optical LO to generate the THz beat signal. Note that the Tx LO refers to a single laser line whereas the aforementioned Rx LO is the beating of two laser lines. The current contribution according to ii) is referred as Tx data current (I_{Mod}). To quantify the impact of the current ratio and the total photocurrent on the signal quality, we measure the bit-error-ratio (BER) while keeping the other parameters fixed. In particular, the carrier frequency is f_{THz} =120 GHz, the IF is f_{IF} =8 GHz, the optical power at the Rx is $P_{opt,Rx}$ = 40 mW, and the gross data rate is 10 Gbit/s.

The results are shown in Fig. 7. The intensity of the beat signal is highest for balanced optical signals, i.e. when I_{LO} equals I_{TX}. The lowest BER, however, is achieved when I_{Mod} is significantly lower than I_{LO}. We explain this by the presence of spurious signals in the IF spectra, which we observed even when turning off the optical excitation at the Rx. Fig. 8 shows the IF spectra captured from the RTO for two different data currents in the transmitter when the Rx is turned on and off. When the Rx LO beating is on, the spectrum of the 10 Gbit/s down-converted data signal can be seen. However, even without the Rx LO, strong peaks are present in the spectrum which likely stem from the direct detection (envelope detection) of the phase-modulated optical data signal on the transmitter PIN diode, resulting in an unmodulated pulse train with a line spectrum at IF frequencies. This spurious signal is emitted from the Tx, transmitted to the receiver antenna and directly passed through to the amplifier. Although the antennas employed in our Tx and Rx are not designed for such low frequencies, they can still act as short dipoles and it appears that this effect is strong enough to significantly reduce the signal to interference plus noise ratio (SINR) of any down converted THz signals. For the subsequent experiments, we choose the Tx LO and data current as 7 mA and 2 mA, respectively, to minimize the BER.

Next, we investigated the influence of the optical LO power at the Rx. The BER obtained for power levels between 15 mW and 40 mW presented in Fig. 9 decreases linearly over the optical power. This is expected, since the IF current depends

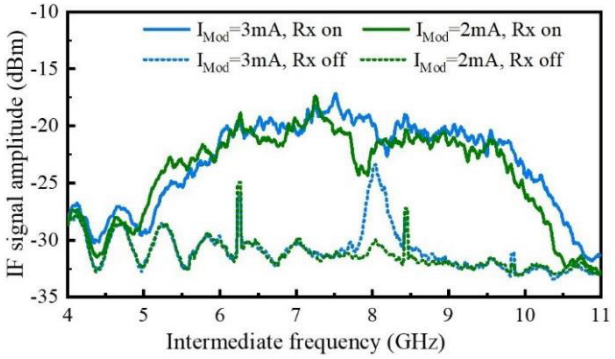

FIGURE 8. IF spectra measured with the RTO when turning the Rx LO on and off. The Tx LO current was set to 7 mA and the data rate was 10 Gbit/s. Even with the Rx turned off, spurious tones from the TX are visible.

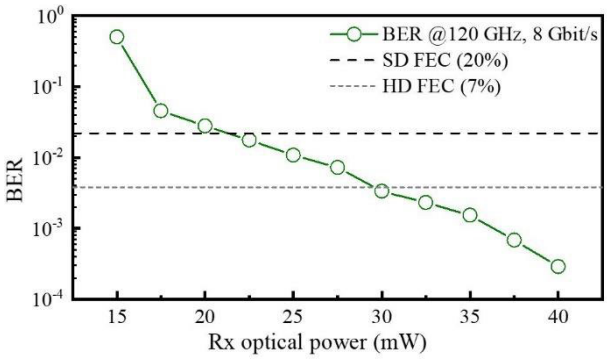

FIGURE 9. Measured BER over the optical LO power at the Rx. The dashed lines indicate the soft decision (SD) and hard decision (HD) forward error correction thresholds. The BER increases faster than linear on a semi-logarithmic scale.

linearly on the photo-conductance, and thus, scales linearly with the optical power (c.f. Fig. 2). The signal power at the load, however, is a function of the square of IF current, as seen in (1). Although these results suggest that higher LO powers at the Rx would further improve the link performance, we limited the optical power to 40 mW to prevent destruction of the device.

2) CARRIER FREQUENCY AND DATA RATE

Using the optimum settings for the Tx and Rx optical inputs obtained from the previous experiments, we subsequently investigated the capabilities of our link for different data rates and carrier frequencies. Fig. 10 shows the measured BER for carrier frequencies from 100 to 320 GHz and gross data rates between 4 and 12 Gbit/s. The BER shows a minimum at 120 GHz which coincides with the maximum of the homodyne spectrum we demonstrated in Fig. 4. Here, we achieved error-free transmission for up to 12 Gbit/s gross data rate using soft-decision (SD) forward error correction (FEC) with 20% overhead (corresponding to 10 Gbit/s net data rate) and for up to 8 Gbit/s gross data rate using hard-decision (HD) FEC with only 7% overhead (corresponding to 7.5 Gbit/s net data rate). For higher carrier frequencies, the BER increases

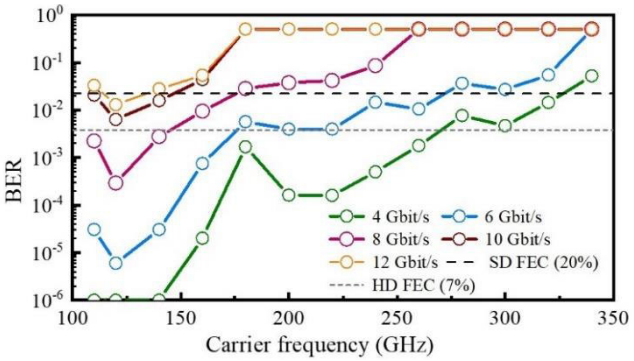

FIGURE 10. Measured BER over carrier frequency for various gross data rates. The optical driving parameters were chosen as described previously and the IF was set to 8 GHz. A BER of 10^{-6} indicates that no errors were found over all received sequences. Error free transmission (below the SD FEC threshold) was achieved up to 320 GHz at 4 Gbit/s gross data rate (3.3 Gbit/s net data rate). A maximum net data rate of 10 Gbit/s was achieved at 120 GHz (12 Gbit/s gross data rate).

as the THz signal amplitude decreases. At 320 GHz, however, we were still able to measure a BER below the 20% FEC limit using a gross data rate of 4 Gbit/s (corresponding to a net data rate of 3.3 Gbit/s). These combinations of carrier frequency and bit rate are record values for full photonic THz links without using a THz amplifier at the receiver.

IV. DISCUSSION

The presented results are a significant improvement over state-of-the-art for both heterodyne PCA THz receivers and full photonic THz links in terms of single channel line rate and IF bandwidth. Our receiver achieved 11 GHz IF bandwidth with an improved THz response over the targeted frequency range from 100 to 300 GHz. Previous works only achieved bandwidths between 37 MHz (IF Bandwidth of the commercially available PCAs used in [16]) and 2 GHz [2], which limited their data rates to between 100 Mbit/s and 10 Gbit/s, respectively, where the latter was only achieved using a THz wave amplifier at the Rx. With our receiver module we were able to achieve error free transmission between 4 and 12 Gbit/s without any THz amplifiers.

In comparison to state-of-the-art electronic mixer based receivers, our technology is not yet competitive. With such devices, IF bandwidths and conversion gains of up to 32 GHz and −15 dB [13], respectively, have been shown, enabling data rates of more than 100 Gbit/s [13], [15]. However, it has to be noted, that the conversion gain reported in such works usually only includes the mixer itself, while our device is directly integrated with the antenna so that the conversion gain measured in this paper also includes the antenna-efficiency and any matching losses between the antenna and the photoconductor.

Although the data rates and IF bandwidths are not yet comparable to electronic receivers, our optoelectronic device has the advantage that it can be used over a very broad band, whereas electronic solutions are typically bound to

smaller waveguide bands. Furthermore we see several ways to improve the performance of PCA-based heterodyne THz detectors to bridge the gap to electronics. First of all, we found the transmission of direct detection components of the optical signal at baseband frequencies by the transmitter to be a strong limitation. This can be alleviated by using different modulation schemes or Antennas and also by increasing the link distance. Furthermore, larger mirrors can increase the gain of both, Tx and Rx to improve the SNR. Previous work on ultrafast photoconductors for 1550 nm has shown the superior properties of InGaAs:Rh for pulsed THz antennas. Currently, InGaAs:Rh is under investigation for cw-THz antennas and we expect an improvement of the conversion gain of at least 18 dB in comparison to the iron-doped PCAs. In combination with optical waveguide-integration of the receivers, which has the potential to increase the conversion gain due to optimized optical coupling, an improvement of the conversion gain of up to 30 dB seems feasible. In addition, in future work we will focus on the HF-design of the heterodyne receiver aiming for IF bandwidths beyond 30 GHz. We therefore believe that PCA receivers can become a viable alternative to electronic THz receivers with a much higher THz carrier bandwidth.

V. SUMMARY AND OUTLOOK

We presented a photonic heterodyne THz receiver, specifically designed for communication applications and employed it in a fully photonic THz link. The THz frequency response of the heterodyne THz receiver is almost identical to state-of-the-art PCAs optimized for spectroscopy, while increasing the IF bandwidth from <37 MHz to 11 GHz. The device showed a peak conversion gain of -47 dB at 40 mW of optical excitation at a carrier frequency of 120 GHz. This enabled us to demonstrate error-free data transmission for data rates between 4 and 12 Gbit/s gross data rates (corresponding to 3.3 and 10 Gbit/s net data rates) at carrier frequencies between 100 and 320 GHz. These results are a significant improvement over state-of-the-art full photonic THz links mentioned in the introduction in terms of carrier frequency, single channel line rate and bandwidth. Compared to the data rates of more than 100 Gbit/s achieved with electronic receivers, which often feature conversion gains greater than -20 dB and IF bandwidths of more than 20 GHz [13], [23], [24], [25], our results are not yet competitive. However, electronic receivers suffer from lower carrier bandwidths so that the spectrum from 100 to 300 GHz could not be addressed with a single electronics-based device. Furthermore, our investigation showed that there is huge potential to improve the link budget of our full photonic links to bridge the gap to electronic links. That is because we found that the BER was mainly limited by spurious tones at IF frequencies, likely stemming from direct detection of the phase-modulated data signal on the PIN photodiode, that were emitted by the Tx antenna. Furthermore, on the Rx side, there is also huge potential to greatly improve the performance of the photonic link. We believe that using rhodium (Rh) doped InGaAs for the absorber, waveguide integrating the receiver and improving the packaging can improve the conversion gain by about 30 dB and the IF bandwidth by 20 GHz. Overall, our work demonstrates that PCAs are promising THz receivers for communications applications, providing full compatibility with the existing fiber-based optical telecommunications infrastructure. To the best of our knowledge, we presented the best performing PCA based THz detector in terms of IF bandwidth and data rate.

REFERENCES

[1] G. Ducournau, P. Szriftgiser, F. Pavanello, E. Peytavit, M. Zaknoune, D. Bacquet, A. Beck, T. Akalin, J.-F. Lampin, and J.-F. Lampin, "THz communications using photonics and electronic devices: The race to data-rate," *J. Infr., Millim., THz Waves*, vol. 36, no. 2, pp. 198–220, Feb. 2015, doi: 10.1007/s10762-014-0112-x.

[2] T. Harter, S. Ummethala, M. Blaicher, S. Muehlbrandt, S. Wolf, M. Weber, M. M. H. Adib, J. N. Kemal, M. Merboldt, F. Boes, S. Nellen, A. Tessmann, M. Walther, B. Globisch, T. Zwick, W. Freude, S. Randel, and C. Koos, "Wireless THz link with optoelectronic transmitter and receiver," *Optica*, vol. 6, no. 8, p. 1063, 2019, doi: 10.1364/optica.6.001063.

[3] C. Castro, R. Elschner, T. Merkle, C. Schubert, and R. Freund, "Long-range high-speed THz-wireless transmission in the 300 GHz band," in *Proc. 3rd Int. Workshop Mobile THz Syst. (IWMTS)*, Jul. 2020, pp. 1–4, doi: 10.1109/IWMTS49292.2020.9166263.

[4] X. Li, J. Yu, J. Zhang, Z. Dong, F. Li, and N. Chi, "A 400G optical wireless integration delivery system," *Opt. Exp.*, vol. 21, no. 16, p. 18812, 2013, doi: 10.1364/oe.21.018812.

[5] L. Moeller, J. Federici, and K. Su, "2.5 Gbit/s duobinary signalling with narrow bandwidth 0.625 terahertz source," *Electron. Lett.*, vol. 47, no. 15, p. 856, 2011.

[6] S. Koenig, "Wireless sub-THz communication system with high data rate," *Nature Photon.*, vol. 7, no. 12, pp. 977–981, Dec. 2013, doi: 10.1038/nphoton.2013.275.

[7] I. F. Akyildiz, A. Kak, and S. Nie, "6G and beyond: The future of wireless communications systems," *IEEE Access*, vol. 8, pp. 133995–134030, 2020, doi: 10.1109/ACCESS.2020.3010896.

[8] T. S. Rappaport, "Wireless communications and applications above 100 GHz: Opportunities and challenges for 6G and beyond," *IEEE Access*, vol. 7, pp. 78729–78757, 2019, doi: 10.1109/ACCESS.2019.2921522.

[9] T. Nagatsuma, G. Ducournau, and C. C. Renaud, "Advances in terahertz communications accelerated by photonics," *Nature Photon.*, vol. 10, no. 6, pp. 371–379, Jun. 2016, doi: 10.1038/nphoton.2016.65.

[10] Y. Liu, B. Zhang, Y. Feng, Z. Niu, C. Qiao, F. Shen, B. Dai, Y. Zhang, and Y. Fan, "10-gbps real-time wireless link over 1.5 km at 220-GHz band based on Schottky-diode transceiver and 16-QAM modulation," *AEU Int. J. Electron. Commun.*, vol. 138, Aug. 2021, Art. no. 153874, doi: 10.1016/j.aeue.2021.153874.

[11] T. Kürner, V. Petrov, and I. Hosako, "Standards for THz communications," in *THz Communications: Paving the Way Towards Wireless Tbps*, T. Kürner, D. M. Mittleman, and T. Nagatsuma, Eds. Cham, Switzerland: Springer, 2022, pp. 503–514.

[12] *IEEE Standard for High Data Rate Wireless Multi-Media Networks-Amendment 2: 100 Gb/s Wireless Switched Point-to-Point Physical Layer*, Standard 802.15. 3D-2017, 2017, pp. 1–55.

[13] H. Hamada et al., "300-GHz. 100-Gb/s InP-HEMT wireless transceiver using a 300-GHz fundamental mixer," in *IEEE MTT-S Int. Microw. Symp. Dig.*, Philadelphia, PA, USA, 2018, pp. 1480–1483, doi: 10.1109/MWSYM.2018.8439850.

[14] I. Kallfass, F. Boes, T. Messinger, J. Antes, A. Inam, U. Lewark, A. Tessmann, and R. Henneberger, "64 Gbit/s transmission over 850 m fixed wireless link at 240 GHz carrier frequency," *J. Infr., Millim., THz Waves*, vol. 36, no. 2, pp. 221–233, Feb. 2015, doi: 10.1007/s10762-014-0140-6.

[15] S. Nellen, S. Lauck, E. Peytavit, P. Szriftgiser, M. Schell, G. Ducournau, and B. Globisch, "Coherent wireless link at 300 GHz with 160 Gbit/s enabled by a photonic transmitter," *J. Lightw. Technol.*, vol. 40, no. 13, pp. 4178–4185, Jul. 2022, doi: 10.1109/JLT.2022.3160096.

[16] A. Morales, G. I. Nazarikov, S. Rommel, C. Okonkwo, and I. T. Monroy, "All-photonic heterodyne sub-THz wireless transmission at 80 GHz, 120 GHz and 160 GHz carrier frequencies," in *Proc. 45th Int. Conf. Infr., Millim., THz Waves (IRMMW-THz)*, Nov. 2020, pp. 1–2, doi: 10.1109/IRMMW-THz46771.2020.9370506.

[17] M. Deumer, S. Breuer, R. Kohlhaas, S. Nellen, L. Liebermeister, S. Lauck, M. Schell, and B. Globisch, "Continuous wave terahertz receivers with 4.5 THz bandwidth and 112 dB dynamic range," *Opt. Exp.*, vol. 29, no. 25, p. 41819, 2021, doi: 10.1364/oe.443098.
[18] S. Nellen, B. Globisch, R. B. Kohlhaas, L. Liebermeister, and M. Schell, "Recent progress of continuous-wave terahertz systems for spectroscopy, non-destructive testing, and telecommunication," *Proc. SPIE*, vol. 10531, pp. 44–51, Feb. 2018, doi: 10.1117/12.2290207.
[19] D. Stanze, T. Göbel, R. J. B. Dietz, B. Sartorius, and M. Schell, "High-speed coherent CW terahertz spectrometer," *Electron. Lett.*, vol. 47, no. 23, p. 1292, 2011, doi: 10.1049/el.2011.3004.
[20] A. Steiger, M. Kehrt, C. Monte, and R. Müller, "Traceable terahertz power measurement from 1 THz to 5 THz," *Opt. Exp.*, vol. 21, no. 12, p. 14466, 2013, doi: 10.1364/oe.21.014466.
[21] S. Nellen, T. Ishibashi, A. Deninger, R. B. Kohlhaas, L. Liebermeister, M. Schell, and B. Globisch, "Experimental comparison of UTC- and PIN-photodiodes for continuous-wave terahertz generation," *J. Infr., Millim., THz. Waves*, vol. 41, no. 4, pp. 343–354, Apr. 2020, doi: 10.1007/s10762-019-00638-5.
[22] R. Elschner, F. Frey, C. Meuer, J. K. Fischer, S. Alreesh, C. Schmidt-Langhorst, L. Molle, T. Tanimura, and C. Schubert, "Experimental demonstration of a format-flexible single-carrier coherent receiver using data-aided digital signal processing," *Opt. Exp.*, vol. 20, no. 27, p. 28786, Dec. 2012, doi: 10.1364/oe.20.028786.
[23] S. Hara, "A 32Gbit/s 16QAM CMOS receiver in 300 GHz band," in *Proc. IEEE MTT-S Int. Microw. Symp. (IMS)*, Honolulu, HI, USA, Jun. 2017, pp. 1703–1706, doi: 10.1109/MWSYM.2017.8058969.
[24] I. Abdo, "A 300 GHz wireless transceiver in 65nm CMOS for IEEE802.15.3D using push-push subharmonic mixer," in *Proc. IEEE/MTT-S Int. Microw. Symp. (IMS)*, Los Angeles, CA, USA, Aug. 2020, pp. 623–626, doi: 10.1109/IMS30576.2020.9224033.
[25] I. Belio-Apaolaza, J. Seddon, D. Moro-Melgar, H. P. Indiran, C. Graham, K. Balakier, O. Cojocari, and C. C. Renaud, "Photonically-driven Schottky diode based 0.3 THz heterodyne receiver," *Opt. Exp.*, vol. 30, no. 24, p. 43223, 2022, doi: 10.1364/oe.471102.

MILAN DEUMER received the B.Sc. and M.Sc. degrees in electrical engineering from the Technical University of Berlin, Germany, in 2016 and 2018, respectively. He is currently pursuing the Ph.D. degree with the Terahertz Sensor and Systems Group, Fraunhofer Heinrich Hertz Institute (HHI), Berlin, Germany. From 2015 to 2019, he was a Student Research Assistant with the Terahertz Sensor and Systems Group, Fraunhofer HHI. At this time, he worked on the characterization of photonic THz sources and detectors and investigated further improvements of the photodiode-based THz emitters for the master's thesis. Afterwards, he joined the Commonwealth Scientific and Industrial Research Organization (CSIRO), Brisbane, QLD, Australia, as a Visiting Researcher, where he worked on kinetic energy harvesting for batteryless IoT devices. His research interests include the development of photoconductive antennas for CW THz detection for spectroscopy and THz communications.

OLIVER STIEWE received the B.Eng. degree in electrical engineering and the M.Eng. degree in information and communications engineering from the Beuth University of Applied Sciences, Berlin, Germany, in 2017 and 2021, respectively. He is currently pursuing the Ph.D. degree in the field of THz communications, with a focus on high capacity point-to-point (P2P) and point-to-multipoint (P2MP) links.

SIMON NELLEN received the B.Sc. and M.Sc. degrees in physics from the Technical University of Berlin, Germany, in 2012 and 2015, respectively. He is currently pursuing the Ph.D. degree in physics with the Fraunhofer Heinrich Hertz Institute (HHI), Berlin. From 2012 to 2015, he was a Student Research Assistant with the Terahertz Sensor Systems Group, Fraunhofer HHI. At this time, he investigated ultrafast photoconductive switches for pulsed terahertz generation and detection for the master's thesis. Afterwards, he joined Fraunhofer HHI as a Research Associate. He is the author of more than 70 publications in peer-reviewed international journals and conferences proceedings and two inventions. His research interests include photonic devices for continuous-wave terahertz generation and detection, monolithically integrated antennas and radio frequency structures, sensing and communication at terahertz frequencies, and photonic integrated circuits for those applications.

SEBASTIAN LAUCK received the B.Sc. and M.Sc. degrees in electrical engineering from the Technical University of Berlin, Germany, in 2017 and 2019, respectively. From 2016 to 2019, he was a Student Research Assistant with the Terahertz Sensors and Systems Group, Fraunhofer Heinrich Hertz Institute (HHI), Berlin, Germany. During this time, he investigated photodiode-based antenna structures for photonic integrated terahertz emitter as part of the master's thesis. Afterwards, he joined Fraunhofer HHI as a Research Associate/Engineer of RF design and packaging of THz devices and photonic modulators and as a Designer of photonic integrated circuits. He is currently a Research Associate with the Fraunhofer HHI. His research interests include photonic devices for continuous wave terahertz generation and detection, RF design and optical packaging of monolithically integrated modulators, and design and simulation of broadband terahertz antennas for sensing and communication.

STEFFEN BREUER received the B.Sc. degree in physics from Durham University, U.K., in 2002, the Dipl.-Phys. degree from Free University Berlin, in 2006, and the joint Ph.D. degree in physics from Humboldt-University and PDI Berlin, in 2011. Then, he joined The Australian National University, Canberra, Australia, as a Postdoctoral Fellow working on nanowire photovoltaics. Since 2013, he has been an Epitaxy Scientist with Fraunhofer IAF, Freiburg, Germany, developing GaN high electron mobility transistor structures. Since 2016, he has been a Molecular Beam Epitaxy Expert of the Terahertz Sensors and Systems Group, Fraunhofer HHI, Berlin, focusing on the growth of high-quality ultrafast photoconductors for optoelectronics. He is the author of more than 80 publications in peer-reviewed journals and conference proceedings. His research interests include ultrafast semiconductors, photoconductive THz sources and emitters, and saturable absorber mirrors for femtosecond pulse laser mode locking.

He is a member of the German Physical Society.

ROBERT B. KOHLHAAS received the M.Sc. degree in physics from Technische Universität Berlin, Germany, in 2016, and the Ph.D. degree from Technische Universität Berlin, focusing on photoconductive antennas for pulsed terahertz (THz) generation and detection, in 2021. Thereafter, he joined the Fraunhofer Institute for Telecommunications, Heinrich Hertz Institute (HHI), as a Research Associate and the Project Manager. Since 2022, he has been the Head of the Terahertz Sensors and Systems Group, Fraunhofer HHI. He is the author of more than 50 publications in peer-reviewed journals and conference proceedings. His research interests include optoelectronic THz sources and receivers, THz communication links, photonically integrated THz systems, and ultrafast photoconductive materials grown by molecular beam epitaxy.

COLJA SCHUBERT received the Dipl.-Phys. and Dr. rer. nat. degrees in physics from Technische Universität Berlin, Berlin, Germany, in 1998 and 2004, respectively. He was an Exchange Student with Strathclyde University, Glasgow, U.K., from 1996 to 1997. During the Dipl. Thesis, from 1997 to 1998, he was with the Max-Born-Institute for Nonlinear Optics and Short Pulse Spectroscopy, Berlin. Since 2000, he has been a member of the Scientific Staff with the Fraunhofer Institute for Telecommunications, Heinrich-Hertz-Institute, Berlin. His research interests include high-speed transmission systems and all-optical signal processing. He is currently heading the Submarine and Core Systems Group, Photonic Networks and Systems Department, and also the Deputy Department Head.

He is a member of the German Physical Society.

ROBERT ELSCHNER (Member, IEEE) received the Dipl.-Ing. and Dr.-Ing. degrees in electrical engineering from Technische Universität Berlin, Germany, in 2006 and 2011, respectively. In 2005, he was with École Nationale Supérieure des Télécommunications, Paris, France. Since 2010, he has been a member of the Scientific Staff and the Project Manager of the Fraunhofer Heinrich-Hertz-Institute, Berlin. His research interests include digital signal processing for high-speed coherent fiber-optical and THz-wireless systems. He is a member of the IEEE Photonics Society and served on the Technical Program Committee of the Optical Fiber Communication Conference.

RONALD FREUND received the M.B.A. degree. He is currently heading the Department Photonic Networks and Systems, Fraunhofer Heinrich Hertz Institute, Berlin, Germany, with a focus on research and business activities in the fields of network design and modelling, high-capacity submarine and core networks, B5G/6G access networks, and satellite and quantum communication systems. He is also leading the Expert Committees on Optical Communications Engineering and Broadband Access of the Information Technology Society (ITG) in Germany. He is a member of the Management Committees of Europe's leading Conference on Optical Communications (ECOC) and the Optics and Photonics Congress (OPIC), Japan. He has authored/coauthored more than 150 scientific publications.

MARTIN SCHELL (Member, IEEE) received the Diploma degree in physics from RWTH Aachen University, Aachen, Germany, in 1989, and the Dr.rer.nat. degree from the Technical University of Berlin, Germany, in 1993. In 1995, he was a Visiting Researcher with The University of Tokyo, Tokyo, Japan. From 1996 to 2000, he was a Management Consultant with the Boston Consulting Group. From 2000 to 2005, he was the Product Line Manager and the Head of Production and Procurement with Infineon Fiber Optics, Berlin. He is currently the Director of the Fraunhofer Heinrich Hertz Institute, Berlin, and a Professor in optic and optoelectronic integration with the Technical University of Berlin. He was a Board Member of the European Photonics Industry Consortium, from 2015 to 2021. He is also the Chairperson of the Competence Network Optical Technologies Berlin/Brandenburg (OptecBB), the Spokesman of the Berlin-Brandenburg Photonics Cluster, and a member of the Photonics21 Board of Stakeholders.